Title
Identifying climate change impacts on surface water supply in the southern Central Valley, California

Authors
Liu, Zhu
Herman, Jonathan D
Huang, Guobiao
et al.

Publication Date
2021-03-01

DOI
10.1016/j.scitotenv.2020.143429

Peer reviewed

Science of the Total Environment 759 (2021) 143429

Contents lists available at ScienceDirect

Science of the Total Environment

journal homepage: www.elsevier.com/locate/scitotenv

Identifying climate change impacts on surface water supply in the southern Central Valley, California

Zhu Liu [a], Jonathan D. Herman [b], Guobiao Huang [c], Tariq Kadir [c], Helen E. Dahlke [a,*]

[a] Department of Land, Air and Water Resource, University of California-Davis, 1 Shields Ave, Davis, CA 95616, USA
[b] Department of Civil and Environmental Engineering, University of California-Davis, 1 Shields Ave, Davis, CA 95616, USA
[c] Modeling Support Branch, Bay-Delta Office, California Department of Water Resources, 1416 Ninth Street, Sacramento, CA 95814, USA

HIGHLIGHTS

- SWAT models are calibrated with both streamflow and ParBal SWE reference data.
- Four climate models (HadGEM_ES, CNRM-CM5, CanESM2 and MIROC5) and two RCPs were compared.
- Rainfall-runoff season is expected to peak 2–4 months earlier under the warming climate.
- High flows are expected to be 3–8 times of historic flows in the future.
- Snow diminishes quicker at high elevations under the RCP 8.5 scenario.

GRAPHICAL ABSTRACT

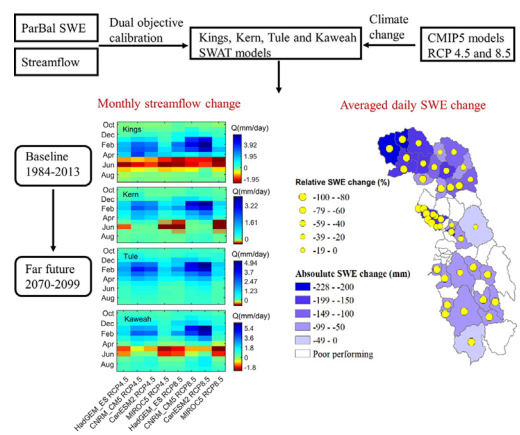

ARTICLE INFO

Article history:
Received 20 August 2020
Received in revised form 15 October 2020
Accepted 15 October 2020
Available online 1 November 2020

Editor: Jay Gan

Keywords:
Surface water supply
Snow water equivalent
SWAT
Multi-objective calibration
CMIP5

ABSTRACT

Mountain regions in arid and semi-arid climates, such as California, are considered particularly sensitive to climate change because global warming is expected to alter snowpack storage and related surface water supply. It is therefore important to accurately capture snowmelt processes in watershed models for climate change impact assessment. In this study we use the Soil and Water Assessment Tool (SWAT) to estimate projected changes in snowpack and streamflow in four alpine tributaries to the agriculturally important but less studied southern Central Valley, California. Watershed responses are evaluated for four CMIP5 climate models (HadGEM_ES, CNRM-CM5, CanESM2 and MIROC5) and two emission scenarios (RCP 4.5 and RCP 8.5) for 2020–2099. SWAT models are calibrated following a dual-objective, lumped calibration approach with an automatic calibration against observed streamflow (stage 1) and a manual calibration against reconstructed Parallel Energy Balance (ParBal) snow water equivalent (SWE) data (stage 2). Results indicate that under a warming climate, peak streamflow is expected to increase 0.5–4 times in magnitude in the coming decades and to arrive 2–4 months earlier in the year because of earlier snowmelt. In the foreseeable future, snow cover will reduce gradually in the lower elevations and diminish at higher rates at higher elevation towards the end of the 21st century. Surface water supply is predicted to increase in the southern Central Valley under the evaluated scenarios but increased temporal variability (wetter wet seasons and drier dry seasons) will create new challenges for managing supply. The study further highlights that the use of remote sensing based, reconstructed SWE data could fill the current gap of limited in-situ SWE observations to improve the snow calibration of SWAT to better predict climate change impacts in semi-arid, snow-dominated watersheds.

* Corresponding author at: Department of Land, Air and Water Resource, University of California-Davis, 1 Shields Avenue, PES 3306, Davis, CA 95616, USA.
E-mail address: hdahlke@ucdavis.edu (H.E. Dahlke).

https://doi.org/10.1016/j.scitotenv.2020.143429
0048-9697/

1. Introduction

Global climate change creates critical challenges to the sustainability of water, energy, food and ecosystem processes at both regional and continental scales (Ashofteh et al., 2017; Ashofteh et al., 2015a; Ashofteh et al., 2015b; Azadi et al., 2019; Conway et al., 2015; Ficklin et al., 2016; Golfam et al., 2019a; Golfam et al., 2019b; Moghadam et al., 2019). Projected impacts of climate change include warmer air temperature, precipitation variability, diminishing snowpack, increased evaporation, and sea level rise (Clark et al., 2016; Flannigan et al., 2016; Huang et al., 2012; Huang et al., 2016; Li et al., 2016; Pachauri et al., 2014; Schmucki et al., 2015; Yin and Tsai, 2018). Extreme precipitation and temperature are projected to intensify in both frequency and severity (Fischer and Knutti, 2015; Wang et al., 2017a). Such changes may trigger a variety of hazards including excessive heat, drought, and flooding, which are disruptive to the environment and economy (Arnell and Gosling, 2016; Liu and Merwade, 2018; Liu and Merwade, 2019; Liu et al., 2019; Oleson et al., 2015; Rajib et al., 2020; Schlaepfer et al., 2017). Alpine watersheds are particularly sensitive to changes in climate since the warmer temperatures are expected to impact the seasonal snowpack, which serves as important reservoir in temperate and semi-arid regions to bridge water availability during the winter rainy season and high water demand during the summer months (Li et al., 2017). Often changes in snowpack in these regions, such as California's Central Valley, directly translate into changes in surface water supply, which can impact water management decisions in downstream regions.

One of the most comprehensive, open source hydrological models available to study hydrologic, biogeochemical or climate change impacts is the semi-distributed Soil Water Assessment Tool (SWAT) (Arnold et al., 1998). SWAT contains a snow module that simulates SWE for defined elevation bands using a temperature-index method and a set of snow calibration parameters. Although these snow parameters could be considered in the calibration process, many SWAT applications in alpine watersheds calibrate the model based on streamflow records only (Lévesque et al., 2008; Rahman et al., 2013; Wang and Melesse, 2005). Omission of considering reference snow data in the model calibration process and only calibrating snow related model parameters with reference streamflow information may not accurately capture the snow storage and snow melt processes that occur in alpine watersheds, resulting in inaccurate projections of snowmelt-driven flow (Bales et al., 2018; Bales et al., 2011; Roche et al., 2019; Zheng et al., 2018). Multi-objective model calibration, where a model is calibrated using two or more reference datasets, is a promising way to improve model performance and reduce parameter equifinality (Parajka and Blöschl, 2008; Yin et al., 2020). Multi-objective model calibration of SWAT has been performed using for example soil moisture or evapotranspiration data in addition to reference streamflow data (Abbaspour et al., 2007; Immerzeel and Droogers, 2008; Rajib et al., 2016), however, the use of snow time series data as the second calibration objective to improve the reliability of calibrated parameter values has been limited (Her and Chaubey, 2015; Rajib et al., 2018; Tuo et al., 2018b), mainly due to the lack of high quality SWE observations (Tuo et al., 2018a).

With the rapid development of measurement devices, remote sensing techniques, and data processing tools, reconstructed SWE datasets are becoming increasingly available for many snow-dominated watersheds (Bair et al., 2018; Brown et al., 2010; Clow et al., 2012; Dozier, 2011; Sturm et al., 2010). Reconstruction of snow water equivalent from remotely sensed data is a technique where the snowpack is built up in reverse from melt-out to peak using downscaled satellite-based energy balance forcings and fractional snow covered area, albedo, and snow grain size data (Bair et al., 2016; Martinec and Rango, 1981). The Parallel Balance Model (ParBal) SWE data is promising reconstructed SWE product available at a daily, 500 m resolution and derived from MODIS Snow Covered Area and Grain Size data (Bair et al., 2016).

The Climate Model Intercomparison Project - Phase 5 (CMIP5) has generated a suite of daily climate forecast datasets for different emission scenarios which are available until the end of the 21st century (Ahlström et al., 2012; Hao et al., 2013; Kumar et al., 2013; Liu et al., 2014; Mehran et al., 2014; Ouyang et al., 2015). These future climate projections can be used to investigate the strain that future climate change imposes on water resource management. In this study, ParBal reconstructed snow water equivalent data and streamflow reference data are used in a dual-objective, lumped calibration of the SWAT model driven by Daymet historical climate data to assess the climate change impacts in four alpine watersheds in the southern Sierra Nevada Mountains. Streamflow and SWE dynamics are predicted for 2020–2099 using precipitation and temperature forcings from four selected CMIP5 models (HadGEM2-ES; CNRM-CM5; CanESM2 and MICROC5) and two emission scenarios (RCP 4.5, 8.5). The specific objectives of our study are to: (1) calibrate SWAT models for four alpine watersheds in the southern Sierra Nevada Mountains using a dual-objective calibration with streamflow and reconstructed SWE reference data; (2) evaluate changes in monthly streamflow and extreme flows in the near (2021–2050) and far future (2070–2099) relative to the historical baseline period; (3) assess spatio-temporal changes in snowpack in each watershed as well as in its vertical distribution across different elevation bands.

The novelty of this study is to evaluate potential climate change impacts on surface water supply in the agriculturally and economically important but less studied southern Central Valley of California, where changes in climate could dramatically reduce the already scarce surface water supply from snow influenced southern Sierra Nevada watersheds (Safeeq and Hunsaker, 2016). Because of the semi-arid climate and importance of the winter snowpack for water supply in the region, we use observed streamflow and reconstructed SWE data in a dual-objective calibration of SWAT to better capture rainfall-runoff and snowmelt dynamics in these watersheds. The dual objective calibration directly addresses the lack of ground based SWE observations and improves the calibration and water supply prediction reliability in these upland watersheds in the coming decades.

2. Study area

This study is focusing on four alpine watersheds, comprised of the Kings (4410 km^2), Kern (5360 km^2), Tule (1400 km^2) and Kaweah (960 km^2) watersheds, in the southern Sierra Nevada Mountains, California, USA (Fig. 1). These rivers drain into the Tulare Lake Basin (TLB), located in the southern Central Valley (CV, 47,000 km^2) of California, one of the most productive agricultural regions in the world (Faunt et al., 2016; Harter and Lund, 2012). The study area was selected because California's CV is an important agricultural region which grows more than 250 different crops and produces more than half of the fruits, vegetables and nuts consumed in the Unites States (Faunt et al., 2009; Faunt et al., 2016; Kocis and Dahlke, 2017) and is heavily dependent on the rainfall-runoff and snowmelt from the Sierra Nevada mountains. The northern part of the CV (Sacramento Basin and San-Joaquin Basin) that drains to the Sacramento-San Joaquin Delta has been studied by many researchers (Ficklin et al., 2013a; Hutton et al., 2019; Thakur et al., 2020) because it provides the majority of surface water supply to California's agriculture using a vast network of surface water conveyance systems. In comparison, local surface water availability in the southern CV, which has the largest farm output ($24.9 billion out of $61.8 billion in 2018; California County Agricultural Commissioners' Reports Crop Year 2017–2018, https://www.nass.usda.gov/) is less studied. Over the last three decades, warmer temperatures have especially impacted the mountain snowpack in the Sierra Nevada Mountains, pushing its center of mass to higher elevations and its snowmelt peak earlier into the spring season (Huning and AghaKouchak, 2018). These trends are expected to continue in coming decades, leading potentially

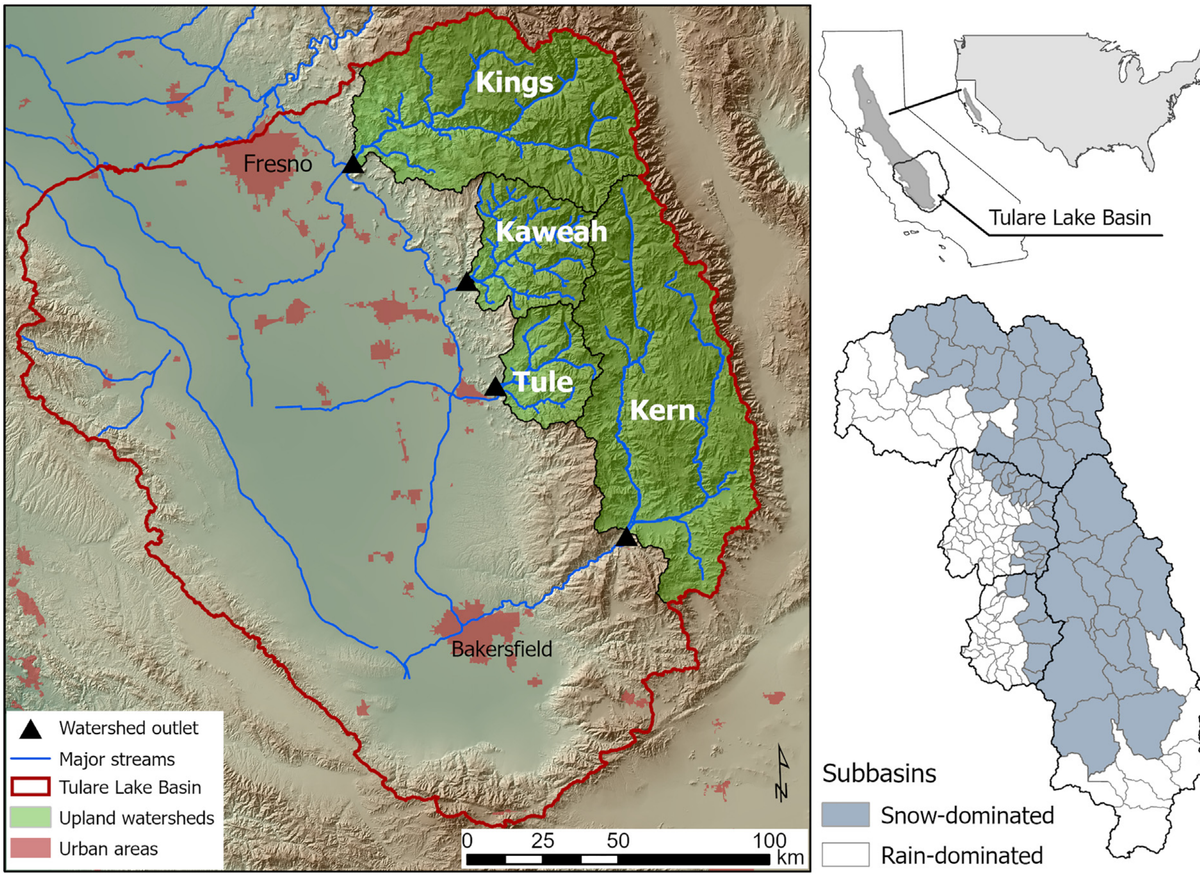

Fig. 1. Location of the four alpine watersheds (Kings, Kern, Tule, and Kaweah rivers) in the southern Sierra Nevada Mountains, California, USA. Snow- and rain-dominated subbasins within each watershed are shown on the right.

to a complete loss of snowpack storage and increased rainfall-runoff from the Sierra Nevada Mountains (Dahlke and Lyon, 2013; Demaria et al., 2016).

The TLB has a Mediterranean to semi-arid desert climate with hot and dry summers and cool and wet winters. Mean annual precipitation can vary between 150 mm in the valley to over 1000 mm in the mountains (Faunt et al., 2016; Lee et al., 2011). The mean annual temperature varies around 18 °C in the study area. But air temperature has been increasing slightly over the past three decades (Fig. S1, Supplementary Materials); mean annual maximum temperature has increased by 0.61 °C whereas the mean annual minimum temperature increased by 1.04 °C during. The main rainy season in the southern Central Valley is from November–March. In some years, precipitation can occur as early as in October and as late as in June.

Based on the typical precipitation occurrence, this study defined the months October–March as the wet season and the months April–September as the dry season when investigating the hydrological and climate characteristics of the study region. As such, each period represents exactly one half of a water year (Oct–Sept of following year; the wet season is the first half and the dry season the second half). Snow is accumulated during the winter season in the Sierra Nevada Mountains, on the east side of the TLB. Due to their size and location the four watersheds exhibit clear differences in the area typically covered by snow in the winter. The snow-covered area in each watershed is approximately 79%, 69%, 70% and 49% respectively for the Kings, Kern, Tule and Kaweah watersheds. All four watersheds have high flows during the spring snowmelt season, with occasional peak flows also occurring during the summer due to thunderstorms. Low flows typically occur at the end of the summer and during the fall season.

3. Material and methods

3.1. Data

3.1.1. Model calibration data

Daymet (https://daymet.ornl.gov/) historic daily precipitation and temperature data (1 km by 1 km resolution, 1981–2013) were used as climate input data for the calibration of each SWAT model with SWAT-CUP. Referenced unimpaired streamflow calculated from observed reservoir operation data at the four watershed outlets were used in the calibration process. The reference streamflow data was obtained from the California Department of Water Resource (DWR) (http://cdec.water.ca.gov/). The Parallel Energy Balance Model (ParBal) daily reconstructed snow water equivalent (SWE) data was used to calibrate the snow-dominated subbasins in each watershed (Fig. 1) (Bair et al., 2018). The ParBal data is available from the University of California, Santa Barbara at 500 m resolution for the years 2001–2017 (ftp://ftp.snow.ucsb.edu/pub/org/snow/products/ParBal/Sierra/). The gridded ParBal data were extracted for each subbasin in each watershed for the further analysis.

3.1.2. Climate prediction data

Gridded datasets of locally downscaled (LOCA) daily precipitation and maximum and minimum temperature data with a 1/16-degree spatial resolution (~7 km at equator) from four CMIP5 models (HadGEM2-ES; CNRM-CM5; CanESM2 and MIROC5) were used to evaluate the snow and hydrological response in our four watersheds for the years 2020–2099. These four CMIP5 models were recommended by the California Climate adaptation group (Cal-Adapt, https://cal-adapt.org/) as priority models for use in climate change adaptation and water resources planning because they encompass different trajectories of future climate. The four models represent a warm and dry climate scenario (HadGEM-ES), a cool and wet climate scenario (CNRM-CM5), an average temperature and precipitation scenario (CanESM2), and the MIROC5 model, which covers the range of CMIP5 model prediction outputs. Each CMIP5 model considers varying greenhouse gas emission rates resulting from solar forcing, anthropogenic activity, volcanic eruption, emissions of short-lived species and natural and anthropogenic aerosols, also known as Representative Concentration Pathways (RCP). For this study, the RCP 4.5 and 8.5 emission scenarios of each CMIP5 model were considered. These two RCPs are most commonly used by researchers since RCP 4.5 is an intermediate scenario whereas RCP 8.5 is generally taken as the worst-case climate change scenario. In summary, data from eight climate models (4 CMIP5 models $*$ 2 RCPs) were used to force the calibrated SWAT models to estimate future monthly streamflow and daily SWE responses. Daily, gridded CMIP5 datasets were downloaded from the United States Bureau of Reclamation (USBR, https://gdo-dcp.ucllnl.org/downscaled_cmip_projections/). The gridded precipitation, minimum and maximum temperature data were extracted for each subbasin in each watershed and time step for year 2020–2099.

3.2. SWAT model

3.2.1. Model description

In this study, the Soil and Water Assessment Tool (SWAT) (version 2009) (Arnold et al., 1998) was used to simulate the snowmelt and rainfall-runoff response in the Kings, Kern, Kaweah, and Tule River watersheds to climate change. SWAT is a semi-distributed, physically-based model that has been used to simulate the quality and quantity of surface water to predict the environmental impact of land use or land management practices, and climate change (Baker and Miller, 2013; Betrie et al., 2011; Ficklin et al., 2009). A SWAT model was developed for each watershed using ArcSWAT, an ArcGIS tool with a graphical user interface that allows building SWAT models from topography, land use and soil data (Abbaspour et al., 2015; Arnold et al., 2012; Winchell et al., 2013). In ArcSWAT, first each watershed was discretized into subbasins based on topography using a USGS 30 m resolution, 1 arc *sec* Digital Elevation Model (DEM, http://ned.usgs.gov). Topography derived terrain slope was combined with soil and land use data to divide each subbasin further into multiple Hydrological Response Units (HRUs). The soil and land use information were derived from the National Land Cover Dataset 2001 land use database (NLCD, https://www.mrlc.gov/data/nlcd-2001-land-cover-conus) and the State Soil Geographic dataset (STATSGO, https://www.nrcs.usda.gov/), respectively. The delineated subbasins in each watershed are illustrated in Fig. 1. SWAT contains a snow module that uses a temperature-index approach to simulate the solid and liquid phase of precipitation as well as snow storage and snowmelt processes. Users can define up to 10 elevation bands to capture orographic effects on precipitation and temperature in alpine watersheds. In this study, five elevation bands (EB) were defined for each SWAT model. Details on the snow module and snowpack mass balance equations in SWAT are described in the Supplementary Materials (Eqs. (S1)–(S5)).

3.2.2. Model set up, calibration and validation

In SWAT, Hydrologic Response Units (HRUs) are the basic hydrologic units used to compute water balance components. After the water balance computation is performed at the HRU level, it is aggregated at the subbasin level and routed towards the major stream reaches and eventually towards the watershed outlet (Kalcic et al., 2015; White et al., 2011).

Each SWAT model was calibrated using a dual-objective calibration process consisting of two stages (Table 1). First an automatic calibration of 17 model parameters against reference monthly streamflow was performed using SWAT-CUP (Abbaspour et al., 2015) to find a satisfactory but preliminary set of parameters (stage 1, Table 1). The model was driven by Daymet historical climate data to best match reference streamflow observations at the watershed outlets. The simulation was initially conducted for one iteration consisting of 500 simulations after which simulation outcomes were evaluated using standard statistical measures (NSE, R^2, *p* value and r value, details are described in the Supplementary Material). A new iteration is initiated by SWAT-CUP until the performance measures are satisfactory. The 17 parameters and their initial ranges were selected following the SWAT documentation (Arnold et al., 2012) followed by a parameter sensitivity analysis conducted by the California Department of Water Resource for the four watersheds (DWR, 2016). The Sequential Uncertainty Fitting algorithm-version 2 (SUFI-2) in SWAT-CUP was applied in this study to find an optimal set of parameter values by narrowing their pre-defined initial ranges (Abbaspour, 2013; Arnold et al., 2012; Ha et al., 2017). The stage 1 calibration was conducted for water years 1981–2000 for which only reference streamflow and no SWE data were available (Table S1 and Table S2, Supplemental Material). The first three years of the historic simulation period (1981–1983) were used as warm-up period for the model and were therefore excluded from the calibration process. The stage 2 calibration was conducted for water years 2001–2007 and snow parameters (summarized in Table S1) were modified manually until a reasonable fit against daily ParBal SWE data was achieved, while the streamflow prediction was maintained at a satisfactory level (NSE ≥ 0.5) compared to the reference streamflow data. The calibrated parameters from stage 2 were evaluated during the validation period (2008–2013) with both streamflow and SWE reference data to prove their suitability for forecasting both variables for future years. After the dual-objective calibration and validation, the calibrated SWAT models were used for forecasting watershed responses to different climate scenarios. The entire model setup, calibration and prediction processes are described in Fig. 2.

Table 1
Dual-objective (two-stage) model calibration and validation and selected forecasting periods and corresponding model objectives.

Modeling	Stage 1	Stage 2	Validation	Forecasting
Period	1981–2000	2001–2007	2008–2013	2020–2099
Objective	Calibration of flow	Calibration of SWE	Validation of flow and SWE	Prediction of flow and SWE

The periods selected for calibration and validation were based on the availability of reference flow and SWE data for the four watersheds. Additionally, the occurrence of both wet and dry years was considered in defining the calibration and validation periods. Streamflow was calibrated and predicted at a monthly time step in SWAT whereas SWE was calibrated at a daily step.

3.3. Analysis of model outputs

3.3.1. Evaluation of climate change impact on streamflow

Monthly water yield (i.e. streamflow normalized by catchment area) was estimated for the outlet of each watershed for the years 2020–2099 for each of the 8 climate scenarios. For each time step the ensemble mean was calculated as the arithmetic mean of the predicted streamflow of the 8 modeling scenarios. In order to quantify the degree to which future changes in climate forcing impact the hydrological response in each watershed, the forecasted streamflow was split into two 30-year periods, the near future (NF, 2021–2050) and the far future (FF, 2070–2099), for comparison with the historical period of 1984–2013 for each modeling scenario. In this comparison, a positive value indicates increasing flow in the future and a negative value indicates decreasing flow in the future. Because severe droughts and floods are both major water resources concerns in California (Diffenbaugh et al., 2015; Griffin and Anchukaitis, 2014), the frequency and

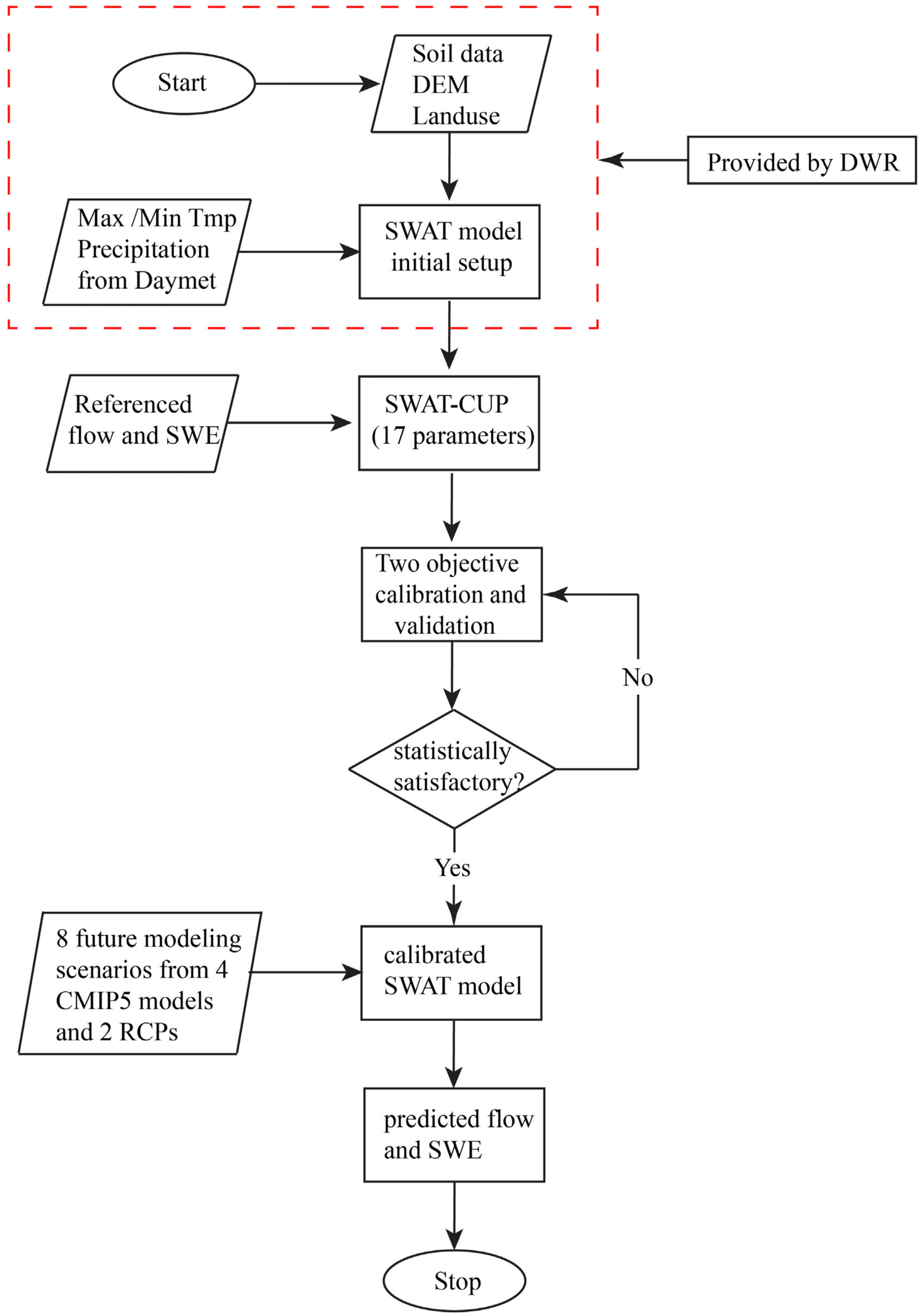

Fig. 2. Flow chart of SWAT model calibration, validation and climate change impact prediction.

magnitude of such events is assessed in the coming decades. Changes in both low (10th percentile, Q10 and 20th percentile, Q20) and high flows (80th percentile, Q80, 90th percentile, Q90, and maximum flow) are evaluated for each modeling scenario and watershed during the wet season (Oct–Mar) and dry season (Apr–Sep), respectively, and compared with the corresponding periods in the historical period (1984–2013).

3.3.2. Evaluation of climate change impact on SWE

Similar to streamflow, SWE is predicted for the 8 climate scenarios for 2020–2099 with the SWAT models and evaluated for the snow calibrated subbasins in each watershed. In order to evaluate the impact of climate change on SWE, the 10-year average daily SWE was calculated for each snow calibrated subbasin for the historical baseline period (2004–2013), the near future (2031–2040) and far future

(2081–2090), respectively. The near and far future periods for the SWE comparison were chosen to be exactly the middle 10 years of the two 30-year periods used for the streamflow comparison. The difference between the near future and baseline, the far future and baseline, as well as the far future and near future were calculated for each snow-dominated subbasin in each watershed for each modeling scenario. In this comparison, a positive value indicates an increase in SWE in the future and a negative value indicates a decreasing trend of SWE in the future.

In addition to assessing the spatial SWE change at the subbasin scale, the projected SWE was also investigated vertically across different elevation bands. The 10-year daily average SWE was evaluated at 5 predefined elevation bands for the near (2031–2040) and far future (2081–2090) in each watershed to determine how snow accumulation is changing vertically from the base to the top of the watershed in the different modeling scenarios.

4. Results

4.1. Two-objective calibration and validation results

During stage 1 of the calibration (streamflow calibration), the model performance achieved by the best set of calibration parameters for all four watersheds ranged between 0.81 and 0.9 (R^2) and 0.7–0.89 (NSE), respectively (Fig. 3, Table S2). Additionally, in the last iteration of the 500 simulations, 65%–97% of the measured data were bracketed by the 95PPU (p value) and r values ranged from 0.67–1.45. Simulated streamflow during the calibration period was higher for the Kings and Kaweah watersheds (i.e. high flows during spring seasons could reach 9 mm/day for Kings and 5 mm/day for Kaweah), which are located closer to the High Sierras and thus experience more snow and snowmelt runoff (Fig. 3). In comparison, the Kern and Tule watersheds are located in the relatively warmer, southern region of the Sierra Nevada Mountains. High streamflow events in these watersheds reach around 2–3 mm/day. After the two-objective calibration both the R^2 and NSE were found to perform slightly lower than after the stage 1 (streamflow only) calibration (i.e. for Kings watershed, the R^2 and NSE reduced from 0.9 and 0.89 after the stage 1 calibration to 0.86 and 0.76 respectively after the stage 2 calibration). This outcome is the result of finding a suitable calibration parameter set for both streamflow and SWE reference datasets. Although the streamflow simulation performance decreased slightly during the stage 2 calibration, the R^2 and NSE values achieved by the model were still very satisfactory (R^2 ranged from 0.59–0.86 and NSE ranges from 0.58–0.78 for the stage 2 calibration period, 2001–2007). After the stage 2 calibration, the model captured rainfall-runoff and snow-runoff processes in all four watersheds more realistically, which reduced the chance of model parameter equifinality. A similar model performance was achieved for the validation period (2008–2013).

NSE values for the snow-dominated subbasins ranged between 0.36 and 0.71 in the Kings watershed after the stage 1 calibration (Fig. 4). After the manual snow parameter calibration was performed in stage 2, model performance in snow-dominated subbasins in the Kings watershed showed a clear improvement in comparison to the reference SWE data (NSE ranged between 0.53 and 0.76). NSE values of the SWE simulation likewise improved substantially in most subbasins in the Kern, Kaweah and Tule watersheds (median NSE values of all subbasins reached 0.65, 0.65, 0.1, 0.55 for the Kings, Kern, Tule and Kaweah watersheds). The Tule watershed, which has the least snow cover and the smallest number of snow-dominated subbasins among the four watersheds also improved slightly after the stage 2 calibration (median NSE increased from 0.05 and 0.1 with some subbasins reaching NSEs of 0.4–0.6). This might indicate that the standard snow module in SWAT does not simulate small amounts of SWE well and/or it might have problems simulating SWE in small, steep watersheds. In addition, some snow-dominated subbasins did not achieve a satisfactory NSE value despite the snow calibration (see red colored subbasins in Fig. 4). Poor model performance in these subbasins might be because of their distinct geographical and climatic features (i.e. northeastern aspect away from main weather pathways). The lumped calibration could not find a calibration parameter set that resulted in high NSEs in all subbasins. However, in general, the simulated SWE in most snow influenced subbasins was much improved. The well calibrated subbasins (blue subbasins in Fig. 4) were used to study future climate change impacts in our four watersheds while subbasins with poor SWE calibration performance (red color) were excluded from future forecasting analysis.

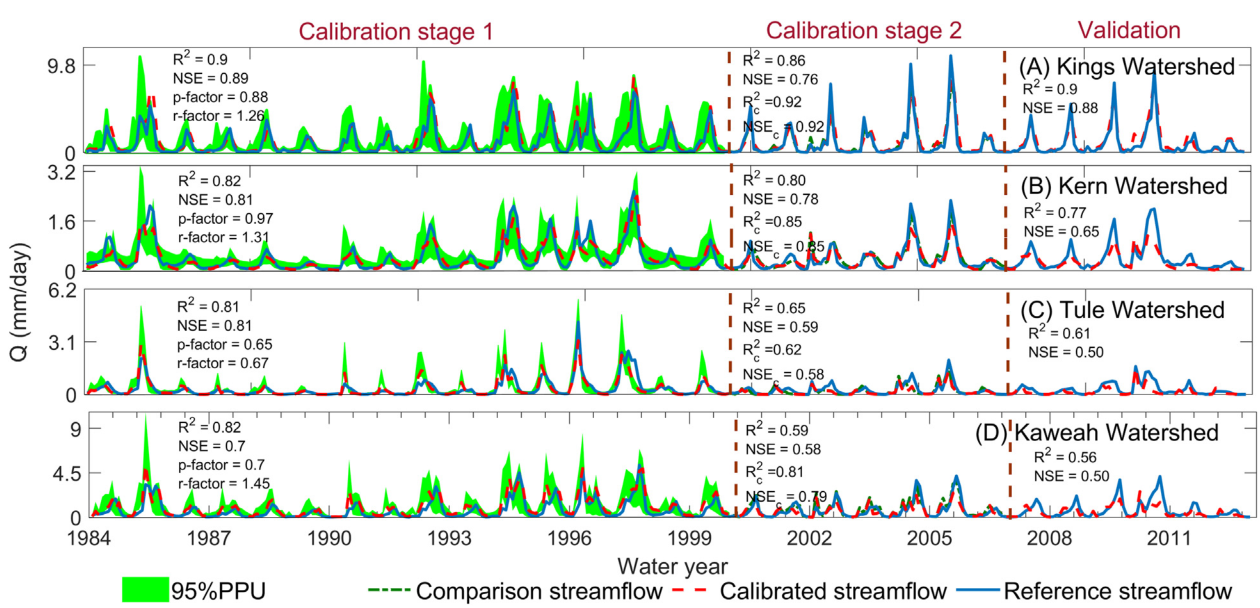

Fig. 3. Simulated streamflow and reference streamflow for calibration stage 1 (1984–2000), calibration stage 2 (2001–2007), and the validation period (2008–2013). Model performance measures (NSE and R^2) are shown for each period. NSE_c and R_c^2 indicate the model performance after the stage 1 calibration before the calibrated parameters from stage 1 were directly applied to the stage 2 snow calibration.

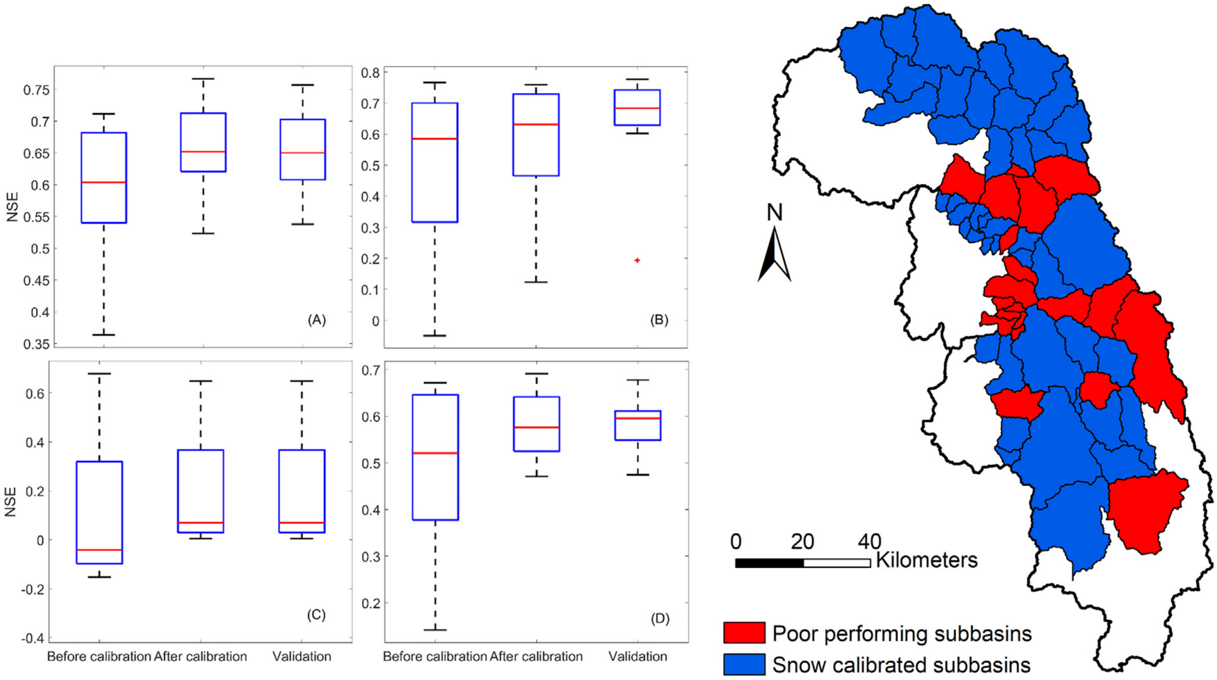

Fig. 4. Distribution of Nash-Sutcliffe Efficiency between the SWAT-predicted and ParBal-observed SWE across all snow-dominated subbasins within the Kings (A), Kern (B), Tule (C), and Kaweah (D) watersheds. The NSE distribution is shown before and after the stage 2 calibration (snow calibration) as well as for the validation period. Subbasins in which the snow calibration performed poorly are indicated in red. These subbasins had an NSE of <0.52, < 0.12, <0.004, and <0.47 in the Kings, Kern, Tule, and Kaweah watershed, respectively and were excluded from the climate change forecast analysis.

4.2. Projected climate change and its impact on streamflow

The four climate models and two RCP scenarios predict an increase in air temperature in all four watersheds in the coming decades (Fig. S2 in the Supplementary Materials). In comparison, precipitation is projected to either increase or slightly decrease depending on the watershed. Compared to the mean annual maximum temperature in the historical period (1984–2013), different climate trajectories show that in the far future (2070–2099) the annual maximum air temperature changes by approximately 0.5–7.5 °C, 1–7 °C, −1.5-4 °C and 0.2–7 °C relative to the historical mean annual maximum temperature in the Kings, Kern, Tule and Kaweah watersheds, respectively. The mean annual minimum temperature changes by about 0–5 °C, −0.5–4.5 °C, −2.5–3 °C and −0.5–4.5 °C relative to the historical mean of the annual minimum temperature in these four watersheds. Similarly, the change of total annual precipitation in the far future relative to the historical mean ranges between −558-1752 mm (−60%–200%), −398-1346 mm (−70%–230%), −327–1751 mm (−60%–300%) and −687–1371 mm (−70%–140%) respectively in the Kings, Kern, Tule and Kaweah watersheds, reflecting the disagreement of climate models on projected precipitation change in California (Berg and Hall, 2015).

There exists substantial inter-model variability in the predicted future flow, reflecting the differences in the climatic forcing represented by the different climate models (Fig. 5A1–D1). As expected, the cool and wet CNRM-CM5 climate model predicts higher peak flows in the coming decades (i.e. 18 mm/day around 2025 for Kings under RCP 4.5). Under the CNRM-CM5 RCP 8.5 emission scenario extreme flows are predicted to become more severe (i.e. 21 mm/day around 2090 for Kings with RCP 8.5), resulting in at least a three-fold increase in peak flows in all watersheds. In comparison, ensemble mean predictions from all other climate scenarios are predicted to reduce flow peaks in the hydrograph. High flows are projected to increase in the future both during wet and dry seasons in all four watersheds. Extreme events (e.g. flows >90th percentile), which might trigger flooding, could increase 3–8 times in magnitude during wet seasons compared to the historical baseline period. For instance, under the CNRM-CM5 RCP 8.5 climate scenario, the Kings River maximum monthly flow is predicted to increase fivefold from 3.92 mm/day in the baseline period to about 19.59 mm/day in the future. Even during the dry season the maximum flow peaks are predicted to increase 1.5 to 2 times that of the baseline period for most of the wetter climate scenarios (i.e. increase from 9 mm/day in the baseline period for Kings watershed to 17–18 mm/day for CNRM_CM5 model and 14–16 mm/day for CanESM2 models under RCP 4.5 and RCP 8.5 conditions). In contrast, low quantile (Minimum, 10th percentile, 20th percentile) flows are predicted to see a slight decline or to generally remain on a similar level as observed during the baseline period. Dry season flows in the Kings, Kern and Kaweah watersheds are predicted to decrease by −2.31, −0.35, −2.34 mm/day for the near future and by −2.64, −0.47, −2.43 mm/day for the far future compared to baseline period. Low flows in the Tule watershed, which has the least snow cover of all watersheds, are predicted to remain the same. Overall, our results indicate that all four watersheds will likely reach flooding conditions (e.g. high magnitude flows) more frequently in the future (Fig. 5). This might be because the warmer air temperature predicted in all climate scenarios will lead to more intense snowmelt or rainfall-runoff events in the future.

Mean monthly streamflow is predicted to increase during the wet season (Oct-Mar) in the near (2021–2050) and far future (2070–2099) in all four watersheds (Fig. S3). However, the increase in wet season streamflow is occurring at a lower rate in the far future compared to the near future (Fig. S3A and S3C). For instance, in the Kings watershed averaged monthly streamflow during wet seasons increases by 1 mm/day in the near future compared to the baseline period whereas the increase in the far future is around 0.6 mm/day compared to the near future. As expected, inter-model differences exist between the climate scenarios. Under the CNRM_CM5 and CanESM2 climate scenarios, the SWAT models predict a higher increase in streamflow until the end of this century (i.e. Fig. S3B, E, H and K).

Fig. S3 also shows that the rate of increase differs between the seasons; it is higher for late winter and early spring (January to March) and lower for late fall and early winter (August to December). For instance, for the Kings watershed the increase in streamflow is around 1–2 mm/

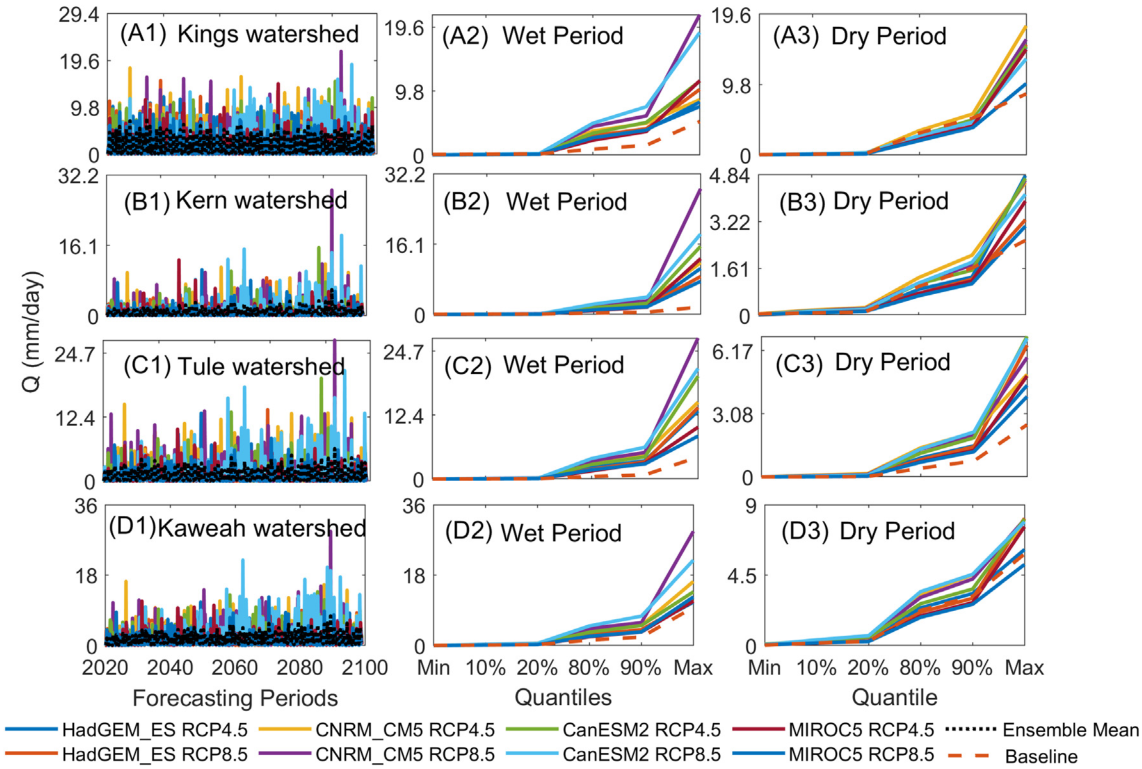

Fig. 5. Monthly streamflow (A1–D1) and selected low flow and high flow quantiles predicted for the wet (A2–D2) and dry seasons (A3–D3) for the four watersheds for 2020–2099. Results are shown for the 8 climate scenarios; baseline period is 1984–2013.

day during January to March in the near future and less than 1 mm/day during August to December. In addition, the timing of high flows is shifting, which are predicted to occur earlier in the future. The seasonal peak in streamflow might come as early as January or February in the future whereas flows peaked around May in the 1980s. The dry seasons are predicted to start earlier in the future as streamflow starts to decline in May for the Kings and Kaweah watersheds. In addition, due to the predicted increase in total annual streamflow and the earlier onset of the wet season (flow starts to increase in December), the low flow periods (i.e. flow <1 mm/day for Kings watershed) are predicted to be shorter in the future. During the 1980s, the low flow period typically lasted from August to February of the following year in the Kings watershed. In the far future the low flow period is predicted to start around July and end in November. However, model differences exist among the eight climate scenarios. For example, the CNRM_CM5 and CanESM2 climate models predict higher flow increases for the future whereas the MIROC5 model predicts the lowest flow increases during the wet seasons for the future.

4.3. Influence of climate change on SWE at the subbasin scale

In the future the absolute amount of SWE reduces significantly (around −50 mm) in the Tule and Kaweah watersheds (Fig. 6). These two watersheds are located in the southern part of the study are and thus will experience relatively more warming than their northern counterparts. SWE is also predicted to decline in the western parts of the Kings and Kaweah watersheds (around −100 mm), which are the lower elevation regions, where snow is easier to melt. The eastern parts of the Kings and Kaweah watersheds are closer to the High Sierras, a region known for its high elevation and large snowpack. Based on the HadGEM_ES model, snowpack will increase slightly in the High Sierras (0–70 mm under RCP 4.5 scenario) in the near future compared to the baseline period (which might be related to the regional climate such as precipitation in that period) and decrease in the far future as the temperature continues to increase (Belmecheri et al., 2016; Huang et al., 2018; Walton et al., 2017). In the far future (2081–2099) the low elevation snowpack will completely disappear, and the high elevation snowpack is increasingly diminishing at higher rates, as indicated by the subbasins in the northern Kings and Kern watersheds (Fig. 6).

There exists a slight inter-model variability with respect to the predicted SWE change (Fig. 7). For instance, the predicted median absolute SWE change for all snow subbasins varies between −80 and 0 mm among climate models for the Kings watershed and between −100 and 0 mm for the Kaweah watershed. Absolute SWE change is less than 50 mm for the Kern and Tule watersheds. SWE is predicted to decrease in most snow-dominated subbasins in the future, which is reflected by the position of the box-whisker plots relative to the "no change" line (0 mm dash line, Fig. 7). In general, the RCP 8.5 emission scenario yields a greater change in SWE in both the near and far future for all four climate models. This indicates that the warming climate is expected to continue to reduce the snowpack in the coming decades. Towards the end of this century, the snowpack is predicted to reduce to 10%–60% of the baseline conditions. Especially for the Kern and Tule watersheds, which are located in the southern Sierras, the snowpack will, on average, reduce by 70% in each subbasin. This might be due to a combination of different effects and feedback mechanisms that anthropogenic global warming exerts on snow and the local hydrological processes. As the snowpack continues to diminish, the reduction in snow covered area will decrease the magnitude of the feedback to the extent that large changes are no longer possible to occur.

4.4. Projected SWE in different elevation bands

With increasing elevation, the amount of snow accumulation increases in both the near and far future, reflecting a similar pattern as does currently exist in the Sierra Nevada Mountains (Fig. 8). Each watershed has a characteristic snow accumulation profile, which is a function of the total elevation difference, total precipitation, and topography in the watershed. In general, the Kern, Tule and Kaweah watersheds show a more linear increase in snowpack with elevation while the Kings shows

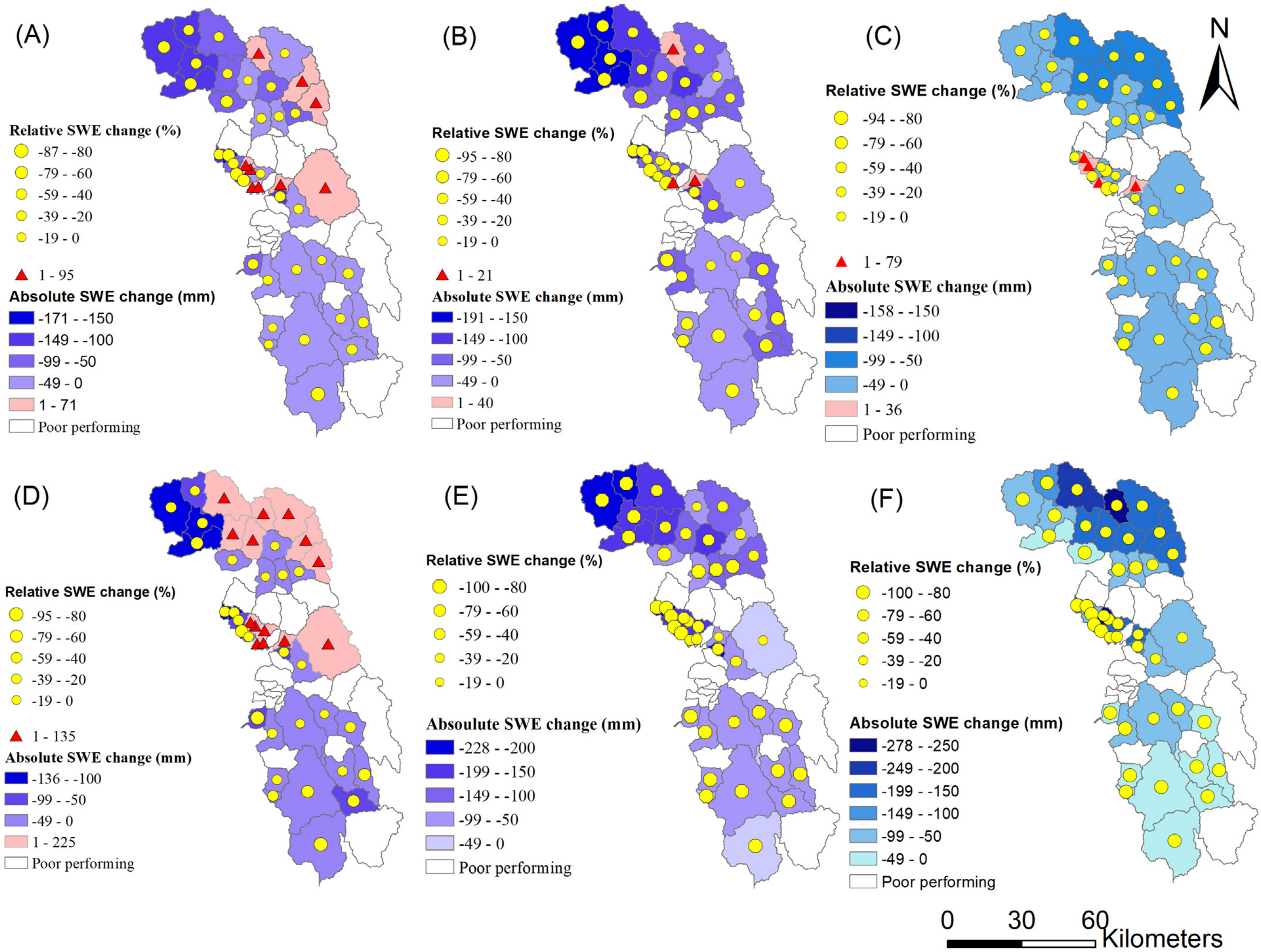

Fig. 6. Comparison of 10-year daily average predicted absolute (mm) and relative SWE (%, circles) change for the HadGEM_ES climate scenario at the subbasin scale. The top row shows the change for the RCP4.5 scenario between the near future (NF, 2031–2040) and the baseline period (2004–2013) (A), the far future (FF, 2081–2090) and the baseline period (B), and the far future relative to the near future (C). The bottom row shows results for the same comparisons under the RCP 8.5 emission scenario.

a slightly exponential elevation profile, indicating that only the very high elevation bands (EB4 & EB5) receive larger amounts of snow. In the near and far future only the highest elevation regions maintain a snowpack (i.e. for Elevation Band 5, 100–200 mm left for Kings, 50–100 mm for Kern, 30–50 mm for Tule and 100–400 mm for Kaweah, Fig. 8). The total SWE predicted for each elevation band varies substantially among the climate models and RCP scenarios. Similar to the spatial trends shown in Figs. 6 and 7, SWE is predicted to decrease more substantially in the far future than in the near future in each elevation band under the same emission scenario. The change in SWE will move the snow line to around 2500 m for the Kings and Kern watersheds and around 2000 m for the Tule and Kaweah watersheds. Similar to the streamflow results presented in this study, the change in SWE across the different elevation bands varies greatly across the different climate models. The cool and wet CNRM-CM5 model, overall predicts higher SWE amounts in each elevation band in the future compared to the other three models.

5. Discussion

5.1. Model performance with streamflow-reconstructed SWE dual-objective calibration

Hrachowitz et al. (Hrachowitz et al., 2016) recently suggested that forcing models to adequately reproduce various response variables can considerably improve the predictive power of models. Degrees of parameter freedom could be controlled towards making better predictions if more observations from measurement, analysis and modeling could be easily assimilated into a model over time (Gupta et al., 2008; Kirchner, 2006). In this study, the two-objective calibration against observed streamflow (stage 1) and remote sensing based reconstructed SWE (stage 2) data resulted in a better model performance than the single-objective calibration using streamflow alone. Although the procedure for model calibration is more complex, as a payoff, model predictions of SWE were much improved while streamflow still performed satisfactory. Using the dual-objective calibration allowed calibration of a model that more accurately represented dominant rainfall-runoff processes in each watershed which reduced the chance of model equifinality (Beven, 2006; Beven and Binley, 1992; Vrugt and Beven, 2018; Vrugt et al., 2009). Using the reconstructed SWE data in the calibration approach particularly increased the calibration efficiency and accuracy for the snow influenced upland watersheds, which is crucial for alpine watersheds.

As mentioned earlier, ground based SWE data could also be used in the SWAT model calibration and validation processes (Tuo et al., 2018b). Dense ground snow measurement networks are desirable because they allow calibration of hydrological models with more details at the subbasin level or for each elevation band. However, not many snow-dominated regions in the world can offer the high station density

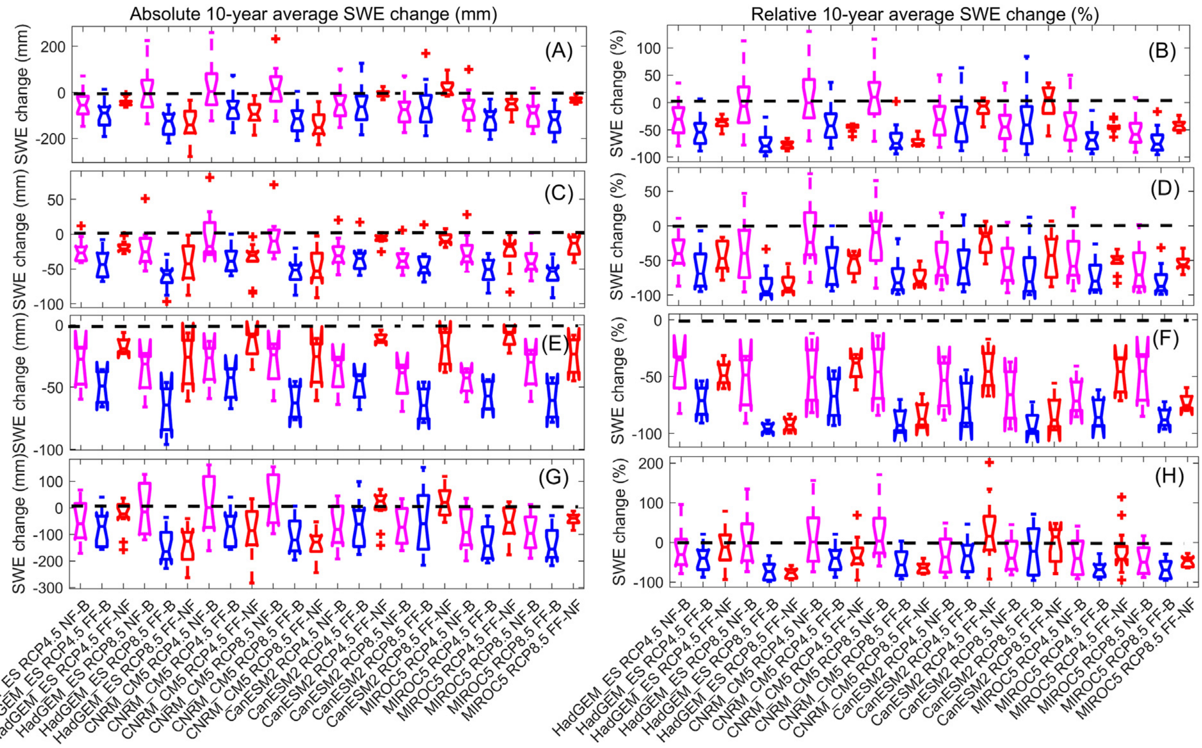

Fig. 7. Distribution of absolute change (mm) and relative change (%) in 10-year daily average SWE in the snow calibrated subbasins for each climate scenario. Box-whisker plots show the change between the far future (FF, 2081–2090), near future (NF, 2031–2040) and the baseline period (B, 2004–2013). A and B show the Kings watershed, C and D the Kern watershed, E and F the Tule watershed, and G and H the Kaweah watershed.

or quality of data needed for model calibration at this time highlighting the need for alternative means of calibrating models with observed SWE data. The reconstructed SWE data used in our study offers a higher spatial and temporal coverage which is particularly appealing for ungauged basins with limited ground-observed data. Recent advances in machine learning techniques now support even the real-time estimation of SWE from remote sensing data (Bair et al., 2018), making the ParBal product available during the snow season for runoff forecasting. We also applied a long calibration period for streamflow (17 years; 1984–2000) and SWE (7 years, 2001–2007) in our study, and applied another 6 years for the SWE and streamflow validation period (2008–2013), which was made possible using the ParBal reconstructed SWE data. Since

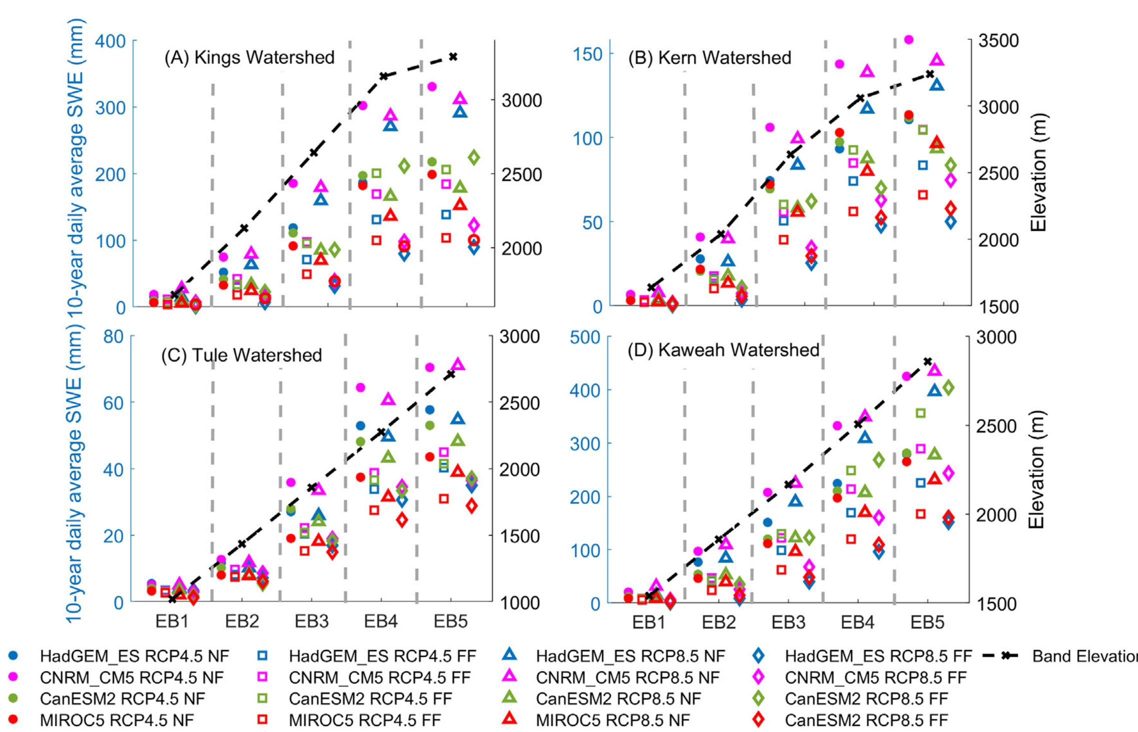

Fig. 8. Comparison of predicted daily average SWE between the far future (2081–2090) and near future (2031–2040) for each elevation band.

California is known for having one of the most variable climates in the entire U.S. (Kocis and Dahlke, 2017), using these long calibration and validation periods ensured that both extremely wet and dry years were included in the calibration and validation periods.

5.2. Comparison of predicted streamflow trends to other studies

The streamflow predictions obtained for the Kings, Kern, Tule and Kaweah watersheds from four climate models and two emission scenarios are generally in line with the findings from previous studies for northern hemisphere mid-latitude alpine watersheds although some regional differences existing among the various basins. Previous climate change studies in the western United States indicate that rising temperatures will result in varied precipitation, reduced snowpack and earlier snowmelt, which likely will increase the frequency and intensity of both drier conditions and flooding events (Esralew et al., 2016; Flint et al., 2013; Pagán et al., 2016). Further, rising air temperatures in winter and spring might lead to earlier snowmelt runoff and a reduction in late spring and summer streamflow (Ashfaq et al., 2013; Barnett et al., 2004). For instance, the shifts in runoff seasonality and timing observed in our study is in line with findings of Gleick and Chalecki (1999), who found in the Sacramento San Joaquin River Basin that during winter (wet period), the risk of winter flooding is likely to increase as the ratio of rain to snow increases and snow melts faster. On the contrary, summer (dry period) water availability is likely to decrease as a result of the earlier ending of spring runoff, which increases the risk of summer water deficits. In a study conducted for the Upper Colorado River Basin (70% of flow originates from Rocky Mountains, Ficklin et al., 2013b), results indicate that summer streamflow declines with median decreases of 46%, and an overall range of −100% to +22%.

In this study, besides the earlier onset of the wet period (wet season flows peak 2–4 months earlier), results indicate that the wet season monthly flow magnitude is projected to increase, while the dry season flow is predicted to decrease (except for the Tule watershed which is predicted to see a general stable trend). This finding indicates that the southern Central Valley will possibly face more challenges of extreme flow events in the future. For the wetter wet seasons, higher flow might result in more frequent flooding events whereas for the drier dry seasons, lower water supply might cause more severe droughts. Both extremes will have strong negative impacts on the agricultural production in the Central Valley and likely result in cause great economic loss as seen during the 2012–2016 drought (Howitt et al., 2014). Thus, adaptation measures and regulation (such as expanding storage to capture surface water during the wet season for use during the dry season) should be taken in the future to minimize the economic loss (Kocis and Dahlke, 2017).

5.3. Comparison of predicted SWE trends to other studies

Similar to our research, previous studies show that the warmer climate projections predict snowpack loss by the end of the century which would significantly affect the agricultural water supply and hydropower production in the western United States (Kapnick et al., 2018; Vicuña et al., 2011). In California, snowpack loss and changes in snow accumulation are predicted to be most severe in the climate projections under the highest emission scenarios (Cayan et al., 2008; Gergel et al., 2017; Kim et al., 2015). Findings from a recent study performed over the southern California mountain region predicts that winter snowfall will be about 70% of baseline by 2050 under the RCP 8.5 scenario and about 80% of baseline for RCP 2.6 scenario (Sun et al., 2016). However, the two different emission scenarios would diverge significantly by the end of the century. A further decline to 50% of baseline snowfall was predicted under the RCP 8.5 scenario whereas the reduction is negligible from 2050 to 2100 under the RCP 2.6 scenario. These findings are generally in accordance with the results obtained in this study with the SWE decreasing amount slightly varying among the four watersheds and climate models. For instance, SWE is predicted to reduce 40–70% in the far future in the Kings watershed whereas a 50–80% reduction is predicted for the Kern watershed. The RCP 8.5 emission scenario would cause a more severe snowpack loss compared to the RCP 4.5 emission scenario until the end of the 21st century.

Moreover, SWE changes are predicted to differ depending on elevations (Mote et al., 2005). For example, Sun et al. (2016) predict for the California mountain region that at low elevation the remaining SWE will be as low as 26%, while about 54% are predicted to remain at moderate elevations. Ensemble-mean midcentury remaining snowpack is predicted to be about 90% of baseline snowpack in the southern California mountains at very high elevations (Sun et al., 2016). These findings have a similar trend to what we concluded in this study. Our results indicate that SWE could reduce by about 40–80% in most subbasins in the four upland watersheds in the far future and that the snow loss mainly comes from the lower elevation bands (Fig. 8) and almost no SWE left for low elevations for the far future. Thus, the temperature changes will also result in a progressively higher snowline in our upland watersheds and only the higher elevation bands (EB4 & EB5) will sustain a winter snowpack for longer periods in the far future.

6. Conclusions

This study evaluated the impact of four CMIP5 climate models (HadGEM-ES, CNRM-CM5, CanESM2 and MIROC5) and two emission scenarios (RCP 4.5 and RCP 8.5) on streamflow and snow water equivalent dynamics in four watersheds located in the southern Sierra Nevada Mountains in California. Climate change impacts were assessed with the Soil and Water Assessment Tool (SWAT) using a dual-objective calibration strategy and monthly streamflow and daily ParBal reconstructed snow water equivalent data. Our results indicate an overall increasing trend in total discharge in all watersheds and all scenarios in the near future and a decline in snowmelt contributions in the far future. However, the impact of climate change on streamflow and SWE is spatially and temporally highly heterogeneous in the four watersheds. Based on our analysis, the following conclusions can be drawn from this study:

1. The use of both reference streamflow and reconstructed SWE in the SWAT model calibration improves the overall prediction reliability for watersheds dominated by rain and snow. Addition of ParBal reconstructed SWE data in the second stage of the calibration process significantly improved the accuracy of the SWE simulation (i.e. NSEs of different subbasins for the Kings River improves from range 0.36–0.71 to range 0.53–0.76) and reduced the likelihood of equifinality issues.
2. The four climate models and two RCP scenarios predict an increase in air temperature and varied precipitation for the four watersheds in the coming decades. In the far future (2070–2099), the annual maximum/minimum air temperature changes by approximately 0.5–7.5 °C/0–5 °C, 1–7 °C/−0.5–4.5 °C, −1.5–4 °C/−2.5–3 °C and 0.2–7 °C/−0.5–4.5 °C relative to the historical baseline period (1984–2013) whereas the change of total annual precipitation ranges between −558–1752 mm (−60%–200%), −398–1346 mm (−70%–230%), −327–1751 mm (−60%–300%) and −687–1371 mm (−70%–140%), respectively in the Kings, Kern, Tule and Kaweah watersheds.
3. High flows are predicted to increase 3–8 fold during the wet season compared to the historical baseline period. This might be because the warmer air temperature will cause more snowmelt, rain on snow, and rainfall-runoff events in the future. The rate of increase differs between the seasons. It is higher for late winter and early spring (1–2 mm/day during January to March in the near future for the Kings watershed) and lower for late fall and early winter (<1 mm/day during August to December). The timing of flow peaks is predicted to occur earlier in the future (Jan. - Mar. in the far future vs. May in the 1980s) and low flow periods are predicted to be shorter in the future. Among the four climate scenarios tested

in this study, the CNRM-CM5 and CanESM2 models with the RCP 8.5 emission scenario predict the highest flow increase during the wet season. Thus, surface water supply in the southern Central Valley might be more challenging in the future because of wetter wet seasons and drier dry seasons.

4. Based on the output from the HadGEM-ES model, the absolute SWE amount is predicted to decrease significantly in the Kern and Tule rivers (around −50 mm in the near future). The low elevation areas on the western slope of the Kings and Kaweah watersheds are predicted to experience snowpack loss of around −100 mm in the near future. In the far future, snowpack diminishes in nearly all subbasins, with an estimated 10%–60% remaining at the end of the century. Only the highest elevation areas (EB4 & EB5) are predicted to maintain a snowpack in the far future. As a result, the snow line will move up to around 2500 m for Kings and Kern watersheds and around 2000 m for Tule and Kaweah watersheds.
5. In general, climate change has a similar influence on the southern Sierras as is found in other northern hemisphere, mid-latitude alpine watersheds. This study highlights that the higher elevation watersheds (Kings and Kern and Kaweah watersheds) will experience drier late spring and early summers while the lower elevation watersheds (Tule) might not suffer from severe summer water supply shortage in the future.

There exist certain limitations for this study. We employed a manual, lumped calibration approach in the snow calibration process. The lumped snow calibration led to the fact that not all snow-dominated subbasins could be calibrated very well resulting in some poorly performing snow-dominated subbasins. Regardless of the limitations, the parameter values derived with the two-objective calibration have improved the SWE performance of the SWAT models, reduced the chance of model equifinality, and increased the reliability of the models for future predictions. Further investigation could focus on implementation of an automatic calibration process for the snow parameters against observed ParBal SWE data at subbasin level to improve the performance of SWAT for future climate change studies.

CRediT authorship contribution statement

Zhu Liu: Conceptualization, Methodology, Software, Writing - original draft. **Jonathan D. Herman:** Validation, Supervision. **Guobiao Huang:** Data curation, Writing - review & editing. **Tariq Kadir:** Supervision, Writing - review & editing. **Helen E. Dahlke:** Conceptualization, Project administration, Funding acquisition, Writing - original draft, Writing - review & editing.

Declaration of competing interest

The authors declare that they have no known competing financial interests or personal relationships that could have appeared to influence the work reported in this paper.

Acknowledgements

This work was supported by the U.S. National Science Foundation (#1716130) and the USDA National Institute of Food and Agriculture, Hatch project CA-D-LAW-2243-H. Authors want to thank Dr. Ned Bair and Dr. Jeff Dozier from the University of California-Santa Barbara for providing the daily ParBal dataset as historical SWE reference. Authors also appreciate editors and two anonymous reviewers for providing constructive suggestions for the earlier version of the manuscript.

Appendix A. Supplementary data

Supplementary data to this article can be found online at https://doi.org/10.1016/j.scitotenv.2020.143429.

References

Abbaspour, K.C., 2013. Swat-cup 2012. SWAT Calibration and Uncertainty Program—A User Manual.
Abbaspour, K.C., et al., 2007. Modelling hydrology and water quality in the pre-alpine/alpine Thur watershed using SWAT. J. Hydrol. 333 (2–4), 413–430.
Abbaspour, K.C., et al., 2015. A continental-scale hydrology and water quality model for Europe: calibration and uncertainty of a high-resolution large-scale SWAT model. J. Hydrol. 524, 733–752.
Ahlström, A., Schurgers, G., Arneth, A., Smith, B., 2012. Robustness and uncertainty in terrestrial ecosystem carbon response to CMIP5 climate change projections. Environ. Res. Lett. 7 (4), 044008.
Arnell, N.W., Gosling, S.N., 2016. The impacts of climate change on river flood risk at the global scale. Clim. Chang. 134 (3), 387–401.
Arnold, J.G., Srinivasan, R., Muttiah, R.S., Williams, J.R., 1998. Large area hydrologic modeling and assessment part I: model development 1. JAWRA Journal of the American Water Resources Association 34 (1), 73–89.
Arnold, J.G., et al., 2012. SWAT: Model use, calibration, and validation. Trans. ASABE 55 (4), 1491–1508.
Ashfaq, M., et al., 2013. Near-term acceleration of hydroclimatic change in the western US. Journal of Geophysical Research: Atmospheres 118 (19), 10,676–10,693.
Ashofteh, P.-S., Haddad, O.B., Loáiciga, H.A., 2015a. Evaluation of climatic-change impacts on multiobjective reservoir operation with multiobjective genetic programming. J. Water Resour. Plan. Manag. 141 (11), 04015030.
Ashofteh, P.-S., Haddad, O.B., Marino, M.A., 2015b. Risk analysis of water demand for agricultural crops under climate change. J. Hydrol. Eng. 20 (4), 04014060.
Ashofteh, P.-S., Bozorg-Haddad, O., Loáiciga, H.A., 2017. Impacts of climate change on the conflict between water resources and agricultural water use. J. Irrig. Drain. Eng. 143 (4), 02516002.
Azadi, F., Ashofteh, P.-S., Loáiciga, H.A., 2019. Reservoir water-quality projections under climate-change conditions. Water Resour. Manag. 33 (1), 401–421.
Bair, E.H., Rittger, K., Davis, R.E., Painter, T.H., Dozier, J., 2016. Validating reconstruction of snow water equivalent in C alifornia's Sierra Nevada using measurements from the NASA Airborne Snow Observatory. Water Resour. Res. 52 (11), 8437–8460.
Bair, E.H., Abreu Calfa, A., Rittger, K., Dozier, J., 2018. Using machine learning for real-time estimates of snow water equivalent in the watersheds of Afghanistan. Cryosphere 12 (5), 1579–1594.
Baker, T.J., Miller, S.N., 2013. Using the soil and water assessment tool (SWAT) to assess land use impact on water resources in an East African watershed. J. Hydrol. 486, 100–111.
Bales, R.C., et al., 2011. Forests and water in the Sierra Nevada: Sierra Nevada watershed ecosystem enhancement project. Sierra Nevada Research Institute report 11.
Bales, R., et al., 2018. Spatially distributed water-balance and meteorological data from the rain–snow transition, southern Sierra Nevada, California. Earth System Science Data 10 (4), 1795–1805 (10(4): 1795-1805).
Barnett, T., et al., 2004. The effects of climate change on water resources in the west: introduction and overview. Clim. Chang. 62 (1–3), 1–11.
Belmecheri, S., Babst, F., Wahl, E.R., Stahle, D.W., Trouet, V., 2016. Multi-century evaluation of Sierra Nevada snowpack. Nat. Clim. Chang. 6 (1), 2.
Berg, N., Hall, A., 2015. Increased interannual precipitation extremes over California under climate change. J. Clim. 28 (16), 6324–6334.
Betrie, G.D., Mohamed, Y.A., Griensven, A.v., Srinivasan, R., 2011. Sediment management modelling in the Blue Nile Basin using SWAT model. Hydrol. Earth Syst. Sci. 15 (3), 807–818.
Beven, K., 2006. A manifesto for the equifinality thesis. J. Hydrol. 320 (1–2), 18–36.
Beven, K., Binley, A., 1992. The future of distributed models: model calibration and uncertainty prediction. Hydrol. Process. 6 (3), 279–298.
Brown, R., Derksen, C., Wang, L., 2010. A multi-data set analysis of variability and change in Arctic spring snow cover extent, 1967–2008. Journal of Geophysical Research: Atmospheres 115 (D16).
Cayan, D.R., Maurer, E.P., Dettinger, M.D., Tyree, M., Hayhoe, K., 2008. Climate change scenarios for the California region. Clim. Chang. 87 (1), 21–42.
Clark, P.U., et al., 2016. Consequences of twenty-first-century policy for multi-millennial climate and sea-level change. Nat. Clim. Chang. 6 (4), 360.
Clow, D.W., Nanus, L., Verdin, K.L., Schmidt, J., 2012. Evaluation of SNODAS snow depth and snow water equivalent estimates for the Colorado Rocky Mountains, USA. Hydrol. Process. 26 (17), 2583–2591.
Conway, D., et al., 2015. Climate and southern Africa's water–energy–food nexus. Nat. Clim. Chang. 5 (9), 837.
Dahlke, H.E., Lyon, S.W., 2013. Early melt season snowpack isotopic evolution in the Tarfala valley, northern Sweden. Ann. Glaciol. 54 (62), 149–156.
Demaria, E.M., Roundy, J.K., Wi, S., Palmer, R.N., 2016. The effects of climate change on seasonal snowpack and the hydrology of the northeastern and upper Midwest United States. J. Clim. 29 (18), 6527–6541.
Diffenbaugh, N.S., Swain, D.L., Touma, D., 2015. Anthropogenic warming has increased drought risk in California. Proc. Natl. Acad. Sci. 112 (13), 3931–3936.
Dozier, J., 2011. Mountain hydrology, snow color, and the fourth paradigm. Eos, Transactions American Geophysical Union 92 (43), 373–374.
DWR, 2016. Estimates of natural and unimpaired flows for the Central Valley of California: water years 1922–2014. Report of California Department of Water Resources.
Esralew, R.A., Flint, L., Thorne, J.H., Boynton, R., Flint, A., 2016. A framework for effective use of hydroclimate models in climate-change adaptation planning for managed habitats with limited hydrologic response data. Environ. Manag. 58 (1), 60–75.
Faunt, C.C., Hanson, R.T., Belitz, K., 2009. Chapter a. introduction, overview of hydrogeology, and textural model of California's Central Valley. US Geological Survey Professional Paper(1766).

Faunt, C.C., Sneed, M., Traum, J., Brandt, J.T., 2016. Water availability and land subsidence in the Central Valley, California, USA. Hydrogeol. J. 24 (3), 675–684.

Ficklin, D.L., Luo, Y., Luedeling, E., Zhang, M., 2009. Climate change sensitivity assessment of a highly agricultural watershed using SWAT. J. Hydrol. 374 (1–2), 16–29.

Ficklin, D.L., Luo, Y., Zhang, M., 2013a. Watershed modelling of hydrology and water quality in the Sacramento River watershed, California. Hydrol. Process. 27 (2), 236–250.

Ficklin, D.L., Stewart, I.T., Maurer, E.P., 2013b. Climate change impacts on streamflow and subbasin-scale hydrology in the Upper Colorado River Basin. PLoS One 8 (8), e71297.

Ficklin, D.L., Robeson, S.M., Knouft, J.H., 2016. Impacts of recent climate change on trends in baseflow and stormflow in United States watersheds. Geophys. Res. Lett. 43 (10), 5079–5088.

Fischer, E.M., Knutti, R., 2015. Anthropogenic contribution to global occurrence of heavy-precipitation and high-temperature extremes. Nat. Clim. Chang. 5 (6), 560.

Flannigan, M., et al., 2016. Fuel moisture sensitivity to temperature and precipitation: climate change implications. Clim. Chang. 134 (1–2), 59–71.

Flint, L.E., Flint, A.L., Thorne, J.H., Boynton, R., 2013. Fine-scale hydrologic modeling for regional landscape applications: the California Basin Characterization Model development and performance. Ecol. Process. 2 (1), 25.

Gergel, D.R., Nijssen, B., Abatzoglou, J.T., Lettenmaier, D.P., Stumbaugh, M.R., 2017. Effects of climate change on snowpack and fire potential in the western USA. Clim. Chang. 141 (2), 287–299.

Gleick, P.H., Chalecki, E.L., 1999. The impacts of climatic changes for water resources of the Colorado and Sacramento-San Joaquin river basins 1. JAWRA Journal of the American Water Resources Association 35 (6), 1429–1441.

Golfam, P., Ashofteh, P.-S., Loáiciga, H.A., 2019a. Evaluation of the VIKOR and FOWA multi-criteria decision making methods for climate-change adaptation of agricultural water supply. Water Resour. Manag. 33 (8), 2867–2884.

Golfam, P., Ashofteh, P.-S., Rajaee, T., Chu, X., 2019b. Prioritization of water allocation for adaptation to climate change using multi-criteria decision making (MCDM). Water Resour. Manag. 33 (10), 3401–3416.

Griffin, D., Anchukaitis, K.J., 2014. How unusual is the 2012–2014 California drought? Geophys. Res. Lett. 41 (24), 9017–9023.

Gupta, H.V., Wagener, T., Liu, Y., 2008. Reconciling theory with observations: elements of a diagnostic approach to model evaluation. Hydrological Processes: An International Journal 22 (18), 3802–3813.

Ha, L.T., Bastiaanssen, W.G., van Griensven, A., van Dijk, A.I., Senay, G.B., 2017. SWAT-CUP for calibration of spatially distributed hydrological processes and ecosystem services in a vietnamese river basin using remote sensing. Hydrology and Earth System Science.

Hao, Z., AghaKouchak, A., Phillips, T.J., 2013. Changes in concurrent monthly precipitation and temperature extremes. Environ. Res. Lett. 8 (3), 034014.

Harter, T., Lund, J.R., 2012. Addressing Nitrate in California's Drinking Water: With a Focus on Tulare Lake Basin and Salinas Valley Groundwater: Report for the State Water Resources Control Board Report to the Legislature. Center for Watershed Sciences, University of California, Davis.

Her, Y., Chaubey, I., 2015. Impact of the numbers of observations and calibration parameters on equifinality, model performance, and output and parameter uncertainty. Hydrol. Process. 29 (19), 4220–4237.

Howitt, R., Medellín-Azuara, J., MacEwan, D., Lund, J.R., Sumner, D., 2014. Economic Analysis of the 2014 Drought for California Agriculture. Center for Watershed Sciences University of California, Davis, CA.

Hrachowitz, M., et al., 2016. Transit times—the link between hydrology and water quality at the catchment scale. Wiley Interdiscip. Rev. Water 3 (5), 629–657.

Huang, G., Kadir, T., Chung, F., 2012. Hydrological response to climate warming: the upper feather river watershed. J. Hydrol. 426, 138–150.

Huang, J., Yu, H., Guan, X., Wang, G., Guo, R., 2016. Accelerated dryland expansion under climate change. Nat. Clim. Chang. 6 (2), 166.

Huang, X., Hall, A.D., Berg, N., 2018. Anthropogenic warming impacts on today's Sierra Nevada snowpack and flood risk. Geophys. Res. Lett. 45 (12), 6215–6222.

Huning, L.S., AghaKouchak, A., 2018. Mountain snowpack response to different levels of warming. Proc. Natl. Acad. Sci. 115 (43), 10932–10937.

Hutton, P.H., Chen, L., Rath, J.S., Roy, S.B., 2019. Tidally-averaged flows in the interior Sacramento–San Joaquin River Delta: trends and change attribution. Hydrol. Process. 33 (2), 230–243.

Immerzeel, W., Droogers, P., 2008. Calibration of a distributed hydrological model based on satellite evapotranspiration. J. Hydrol. 349 (3–4), 411–424.

Kalcic, M.M., Chaubey, I., Frankenberger, J., 2015. Defining soil and water assessment tool (SWAT) hydrologic response units (HRUs) by field boundaries. International Journal of Agricultural and Biological Engineering 8 (3), 69–80.

Kapnick, S.B., et al., 2018. Potential for western US seasonal snowpack prediction. Proc. Natl. Acad. Sci. 115 (6), 1180–1185.

Kim, S.B., Shin, H.J., Park, M., Kim, S.J., 2015. Assessment of future climate change impacts on snowmelt and stream water quality for a mountainous high-elevation watershed using SWAT. Paddy Water Environ. 13 (4), 557–569.

Kirchner, J.W., 2006. Getting the right answers for the right reasons: linking measurements, analyses, and models to advance the science of hydrology. Water Resour. Res. 42 (3).

Kocis, T.N., Dahlke, H.E., 2017. Availability of high-magnitude streamflow for groundwater banking in the Central Valley, California. Environ. Res. Lett. 12 (8), 084009.

Kumar, S., Merwade, V., Kinter III, J.L., Niyogi, D., 2013. Evaluation of temperature and precipitation trends and long-term persistence in CMIP5 twentieth-century climate simulations. J. Clim. 26 (12), 4168–4185.

Lee, J., De Gryze, S., Six, J., 2011. Effect of climate change on field crop production in California's Central Valley. Clim. Chang. 109 (1), 335–353.

Lévesque, É., Anctil, F., Van Griensven, A., Beauchamp, N., 2008. Evaluation of streamflow simulation by SWAT model for two small watersheds under snowmelt and rainfall. Hydrol. Sci. J. 53 (5), 961–976.

Li, X., Xie, S.-P., Gille, S.T., Yoo, C., 2016. Atlantic-induced pan-tropical climate change over the past three decades. Nat. Clim. Chang. 6 (3), 275.

Li, D., Wrzesien, M.L., Durand, M., Adam, J., Lettenmaier, D.P., 2017. How much runoff originates as snow in the western United States, and how will that change in the future? Geophys. Res. Lett. 44 (12), 6163–6172.

Liu, Z., Merwade, V., 2018. Accounting for model structure, parameter and input forcing uncertainty in flood inundation modeling using Bayesian model averaging. J. Hydrol. 565, 138–149.

Liu, Z., Merwade, V., 2019. Separation and prioritization of uncertainty sources in a raster based flood inundation model using hierarchical Bayesian model averaging. J. Hydrol. 578, 124100.

Liu, Z., Mehran, A., Phillips, T.J., AghaKouchak, A., 2014. Seasonal and regional biases in CMIP5 precipitation simulations. Clim. Res. 60 (1), 35–50.

Liu, Z., Merwade, V., Jafarzadegan, K., 2019. Investigating the role of model structure and surface roughness in generating flood inundation extents using one-and two-dimensional hydraulic models. Journal of Flood Risk Management 12 (1), e12347.

Martinec, J., Rango, A., 1981. Areal distribution of snow water equivalent evaluated by snow cover monitoring. Water Resour. Res. 17 (5), 1480–1488.

Mehran, A., AghaKouchak, A., Phillips, T.J., 2014. Evaluation of CMIP5 continental precipitation simulations relative to satellite-based gauge-adjusted observations. Journal of Geophysical Research: Atmospheres 119 (4), 1695–1707.

Moghadam, S.H., Ashofteh, P.-S., Loáiciga, H.A., 2019. Application of climate projections and Monte Carlo approach for assessment of future river flow: Khorramabad River Basin, Iran. J. Hydrol. Eng. 24 (7), 05019014.

Mote, P.W., Hamlet, A.F., Clark, M.P., Lettenmaier, D.P., 2005. Declining mountain snowpack in western North America. Bull. Am. Meteorol. Soc. 86 (1), 39–50.

Oleson, K., et al., 2015. Interactions between urbanization, heat stress, and climate change. Clim. Chang. 129 (3–4), 525–541.

Ouyang, F., et al., 2015. Impacts of climate change under CMIP5 RCP scenarios on streamflow in the Huangnizhuang catchment. Stoch. Env. Res. Risk A. 29 (7), 1781–1795.

Pachauri, R.K., et al., 2014. Climate change 2014: synthesis report. Contribution of Working Groups I, II and III to the Fifth Assessment Report of the Intergovernmental Panel on Climate Change. Ipcc.

Pagán, B.R., et al., 2016. Extreme hydrological changes in the southwestern US drive reductions in water supply to Southern California by mid century. Environ. Res. Lett. 11 (9), 094026.

Parajka, J., Blöschl, G., 2008. The value of MODIS snow cover data in validating and calibrating conceptual hydrologic models. J. Hydrol. 358 (3–4), 240–258.

Rahman, K., et al., 2013. Streamflow modeling in a highly managed mountainous glacier watershed using SWAT: the Upper Rhone River watershed case in Switzerland. Water Resour. Manag. 27 (2), 323–339.

Rajib, M.A., Merwade, V., Yu, Z., 2016. Multi-objective calibration of a hydrologic model using spatially distributed remotely sensed/in-situ soil moisture. J. Hydrol. 536, 192–207.

Rajib, A., Merwade, V., Yu, Z., 2018. Rationale and efficacy of assimilating remotely sensed potential evapotranspiration for reduced uncertainty of hydrologic models. Water Resour. Res. 54 (7), 4615–4637.

Rajib, A., Liu, Z., Merwade, V., Tavakoly, A.A., Follum, M.L., 2020. Towards a large-scale locally relevant flood inundation modeling framework using SWAT and LISFLOOD-FP. J. Hydrol. 581, 124406.

Roche, J.W., et al., 2019. Climate, snow, and soil moisture data set for the Tuolumne and Merced river watersheds, California, USA. Earth System Science Data 11 (1), 101–110.

Safeeq, M., Hunsaker, C.T., 2016. Characterizing runoff and water yield for headwater catchments in the southern Sierra Nevada. JAWRA Journal of the American Water Resources Association 52 (6), 1327–1346.

Schlaepfer, D.R., et al., 2017. Climate change reduces extent of temperate drylands and intensifies drought in deep soils. Nat. Commun. 8, 14196.

Schmucki, E., Marty, C., Fierz, C., Lehning, M., 2015. Simulations of 21st century snow response to climate change in Switzerland from a set of RCMs. Int. J. Climatol. 35 (11), 3262–3273.

Sturm, M., et al., 2010. Estimating snow water equivalent using snow depth data and climate classes. J. Hydrometeorol. 11 (6), 1380–1394.

Sun, F., Hall, A., Schwartz, M., Walton, D.B., Berg, N., 2016. Twenty-first-century snowfall and snowpack changes over the southern California mountains. J. Clim. 29 (1), 91–110.

Thakur, B., Kalra, A., Ahmad, S., Lamb, K.W., Lakshmi, V., 2020. Bringing statistical learning machines together for hydro-climatological predictions-case study for Sacramento San joaquin River Basin, California. Journal of Hydrology: Regional Studies 27, 100651.

Tuo, Y., Marcolini, G., Disse, M., Chiogna, G., 2018a. Calibration of snow parameters in SWAT: comparison of three approaches in the upper Adige River basin (Italy). Hydrol. Sci. J. 63 (4), 657–678.

Tuo, Y., Marcolini, G., Disse, M., Chiogna, G., 2018b. A multi-objective approach to improve SWAT model calibration in alpine catchments. J. Hydrol. 559, 347–360.

Vicuña, S., McPhee, J., Garreaud, R.D., 2011. Agriculture vulnerability to climate change in a snowmelt-driven basin in semiarid Chile. J. Water Resour. Plan. Manag. 138 (5), 431–441.

Vrugt, J.A., Beven, K.J., 2018. Embracing equifinality with efficiency: limits of acceptability sampling using the DREAM (LOA) algorithm. J. Hydrol. 559, 954–971.

Vrugt, J.A., Ter Braak, C.J., Gupta, H.V., Robinson, B.A., 2009. Equifinality of formal (DREAM) and informal (GLUE) Bayesian approaches in hydrologic modeling? Stoch. Env. Res. Risk A. 23 (7), 1011–1026.

Walton, D.B., Hall, A., Berg, N., Schwartz, M., Sun, F., 2017. Incorporating snow albedo feedback into downscaled temperature and snow cover projections for California's Sierra Nevada. J. Clim. 30 (4), 1417–1438.
Wang, X., Melesse, A., 2005. Evaluation of the SWAT model's snowmelt hydrology in a northwestern Minnesota watershed. Transactions of the ASAE 48 (4), 1359–1376.
Wang, G., et al., 2017a. The peak structure and future changes of the relationships between extreme precipitation and temperature. Nat. Clim. Chang. 7 (4), 268.
White, E.D., et al., 2011. Development and application of a physically based landscape water balance in the SWAT model. Hydrol. Process. 25 (6), 915–925.
Winchell, M., Srinivasan, R., Di Luzio, M., Arnold, J., 2013. ArcSWAT Interface for SWAT2012: User's Guide. Blackland Research and Extension Center, Texas Agrilife Research. Grassland. Soil and Water Research Laboratory, USDA Agricultural Research Service, Texas, p. 3.
Yin, J., Tsai, F.T.-C., 2018. Saltwater scavenging optimization under surrogate uncertainty for a multi-aquifer system. J. Hydrol. 565, 698–710.
Yin, J., Pham, H.V., Tsai, F.T.-C., 2020. Multiobjective spatial pumping optimization for groundwater management in a multiaquifer system. J. Water Resour. Plan. Manag. 146 (4), 04020013.
Zheng, Z., Molotch, N.P., Oroza, C.A., Conklin, M.H., Bales, R.C., 2018. Spatial snow water equivalent estimation for mountainous areas using wireless-sensor networks and remote-sensing products. Remote Sens. Environ. 215, 44–56.